

Particle number and size of polystyrene-dependent micellar crosslinking polymerization of acrylic acid

Byungsoo Kim,¹ Daesun Hong,² Wenji V. Chang¹

¹Mork Family Department of Chemical Engineering and Materials Science, University of Southern California, Los Angeles, California

²Department of Chemical Engineering, Dankook University, Yongin City, Gyeonggi-Do, Republic of Korea

Correspondence to: W. V. Chang (E-mail: wenji@usc.edu)

ABSTRACT: The effect of the number and size of polystyrene particles and the concentration of ammonium persulfate used as the initiator on the micellar crosslinking polymerization of acrylic acid was studied by real-time monitoring of the storage modulus (G'), the damping factor ($\tan\delta$), and the ratio of the complex modulus (G^*) to the maximum G^* (G^*_{\max}) during 1 h of polymerization. The molar ratio (5.83×10^{-4}) of N,N' -methylenebis-acrylamide to acrylic acid was fixed. Polystyrene particles were prepared by emulsifier-free emulsion polymerization. The diameter of the particles ranged from 233 to 696 nm. The results show that crosslinking polymerization was most effective when 1.31×10^{12} particles were incorporated into the system, while crosslinking polymerization was less effective in the particle-filled system than in the unfilled polymerization system if the particle number was 50% lower or higher. Crosslinking was also more effective with the use of uncrosslinked firmer and larger particles at the fixed particle number, except for the anomalous behavior observed with 696 nm polystyrene particles. Increasing the feed concentration of the initiator resulted in more efficient crosslinking up to a limiting concentration of 0.765 mg mL^{-1} (the molar ratio of initiator to monomer was 8.52×10^{-4}). When this initiator concentration was doubled, the rate of increase of G' in the deceleration phase was slower after the network was formed. © 2015 Wiley Periodicals, Inc. *J. Appl. Polym. Sci.* **2016**, *133*, 42851.

KEYWORDS: crosslinking; kinetics; mechanical properties; polystyrene; radical polymerization

Received 14 June 2015; accepted 21 August 2015

DOI: 10.1002/app.42851

INTRODUCTION

Rubber commercially used as an elastomeric material is treated with multiple additives to offset its inherent limitations. Hydrogels have mechanical properties that are similar to those of a highly swollen elastomer. Recently, several types of fillers have been incorporated into the hydrogels to effectively introduce functionality and to enhance the mechanical properties at the highly water-swollen status, leading to the development of systems such as a graphene-oxide-filled polyacrylamide hydrogel crosslinked by sodium alginate,¹ a nanocomposite hydrogel composed of graphene oxide, polyacrylamide, and carboxymethylmethyl cellulose sodium,² as well as bio-inspired nanocomposite hydrogels with chitosan or glucose.^{3–7}

Thus, to optimize filled hydrogel systems for purpose-built applications, the properties of the filler, bonding of the filler and hydrogel, and the conditions for crosslinking polymerization should be investigated. The key parameters for maximizing the effect of the filler in mechanically enhanced filled hydrogels are the number of bonds and the strength of bonding between

the backbone chain of the hydrogel and the filler surface. These parameters influence the shear properties such as the storage modulus (G'), complex modulus (G^*), and the damping factor ($\tan\delta$) during the crosslinking polymerization.

Incorporation of a filler into the crosslinking system does not always lead to enhanced mechanical properties. The reaction rate has been used as an indicator of the effectiveness of crosslinking in several systems. The reaction rate either increased or decreased in the case of CaCO_3 -filled polyester,^{8,9} decreased in the case of carbon black-filled epoxy,¹⁰ increased, decreased, or remained the same in the case of SiO_2 -filled epoxy,^{11–13} and increased or remained the same in the case of fiber glass-filled polyester¹¹ when compared to the unfilled congeners. However, the common feature in the aforementioned systems is that bonding between the filler and matrix was achieved by physical interactions such as hydrogen bonding or dipole–dipole attraction. It is difficult to induce the formation of covalent bonds (which are an order of magnitude stronger than physical bonds) between the filler and matrix. Thus, polystyrene, which is a low-density organic filler with relatively easily manipulated

properties,¹⁴ has been used as an emulsion comprising the styrene monomer in the particle phase, and expected to be alternatives to conventional fillers as the reaction media for crosslinking polymerization.

The rigidity of polystyrene is intimately related to the dispersity in solution during the crosslinking polymerization. Radicals from the crosslinked molecules can react with styrene monomers on the surface of the particles. In the case of polystyrene crosslinked using divinyl benzene, it would be more difficult for the radicals to penetrate deeply into the particle. The dispersity of polystyrene particles in suspension generally improves as the amount of divinyl benzene is reduced.¹⁵ Thus, uncrosslinked polystyrene particles would be optimal for preventing coagulation between the particles during crosslinking polymerization.

The size effect exerted by polystyrene particles on the mechanical properties of the polymer matrix is significant. At a fixed polystyrene loading, the total surface area of particles increases as the particle size decreases. Accordingly, the probability of bonding between polystyrene and the matrix increases as the particle size decreases. The time required for gelation during crosslinking polymerization is dependent on the particle size of polystyrene. Cai and Salovey¹⁶ monitored the gelation time for a polystyrene-polysulfide (8000 g mol^{-1}) system. The gelation time was 5.5 h for the pure matrix, over 2 h, 1.4 h, and 13 min for the respective matrices filled with 1250, 688, and 315 nm particles (in diameter). The final moduli of the systems increased as the gelation time decreased.

The particle size of polystyrene prepared by conventional emulsion polymerization is about 50 nm in diameter.¹⁷ Despite the small size, there are several associated shortcomings. For example, removal of the surfactant used in the emulsion polymerization is not only difficult, but also results in coagulation,¹⁸ and complete removal of the surfactant is debatable.^{19,20} If the concentration of the surfactant is low, some coagulation occurs and the particle size distribution would be broader. If the concentration of the surfactant is excessively high, many empty micelles would remain after the polymerization process. In this case, it becomes difficult to isolate the effect of the particles only on the crosslinking polymerization.

Particles prepared via emulsifier-free emulsion polymerization (EFEP) with low solid contents (ca. 10%) have been stabilized by sulfate groups on the surface.^{21–23} The size of polystyrene particles can be kinetically controlled in a reproducible manner to generate mono-disperse particles,²⁴ where the surface is not contaminated by the surfactant; however, the size of the resultant particles may be larger than those generated by emulsion polymerization.²⁵ After nucleation, the particles generated by EFEP range from 10 to 24 nm,²⁶ whereas those from emulsion polymerization range from 5 to 10 nm.¹⁷ In EFEP, oligomeric polystyrene radicals produced by the polymerization of hydrophobic styrene with the decomposed water-soluble potassium persulfate initiator act as the surfactant.

In addition to evaluating the preparation of polystyrene particles for use as a filler, chemical incorporation of the filler into the hydrogel during crosslinking polymerization should also be

investigated. If polystyrene particles prepared by EFEP are used as the filler, the crosslinking polymerization process would be termed “micellar crosslinking polymerization”. It is hypothesized that in this process, radicals of hydrophilic oligomers polymerize with hydrophobic monomers on the particle surface. Abdurrahmanoglu *et al.*²⁷ reported the crosslinking polymerization of acrylamide with methylenebis-acrylamide (MBAAm) in the presence of hydrophobes (*N*-butyl-, *N*-hexyl-, *N*-octyl-, or *N,N'*-dihexyl-acrylamide with sodium dodecyl sulfate). The loss modulus of the resulting hardened hydrogels increased remarkably compared to that of the pure acrylamide hydrogel. Hill *et al.*²⁸ compared free-radical linear copolymerization in micellar, homogeneous, and heterogeneous processes using acrylamide and ethylphenylacrylamide as the hydrophobic comonomer. In the micellar process, they confirmed that sequential hydrophobe blocks were successfully formed between the polyacrylamide chains. The viscosity of the copolymer generated in each process was different, i.e., slightly over 10,000 cp in micellar polymerization, over 1000 cp in heterogeneous polymerization, and over 100 cp in homogeneous polymerization. In the micellar system, the hydrophobe was solubilized in the micelle, which was amphiphilic before the polymerization. Homogeneous polymerization progressed with the use of a co-solvent that could solubilize both monomers. In the heterogeneous polymerization, the solvent selectively solubilized one monomer but did not dissolve the comonomer.

Herein, we conducted EFEP of styrene to produce uncrosslinked particles. Even though the size range of the particles exceeds 200 nm, this system is adequate for clarifying the effect of polystyrene particles (as fillers) on crosslinking of the hydrophilic monomer. The size of the polystyrene particles was monitored by scanning electron microscopy (SEM) at different conversion ratios. Acrylic acid was used as a monomer for crosslinking polymerization with MBAAm. The number and size of incorporated polystyrene particles were varied to monitor the effect of these parameters on the rate of crosslinking polymerization. Furthermore, the effect of the concentration of ammonium persulfate (APS) as an initiator was investigated, where the concentration of APS influences the growing radicals in the filled crosslinking system. Crosslinking polymerization with 1.31×10^{12} polystyrene particles was also performed at different frequencies, i.e., 0.1, 0.5, 1.0, and 10 Hz.

EXPERIMENTAL

Materials

Styrene (purity >90%, inhibited with stabilizer, J. T. Baker Chemical Co.) was used after removing the stabilizer by washing with an alkaline solution. Styrene was washed with 10 wt % NaOH dissolved distilled deionized water three times. Potassium persulfate (purity >99%, Aldrich Chemical Co.), sodium hydroxide (NaOH, Mallinckrodt Baker), acrylic acid (anhydrous; 99%, Aldrich Chemical Co.), MBAAm (99%, Aldrich Chemical Co.), and APS (98+%, A.C.S. reagent, Sigma-Aldrich) were used as received.

EFEP of Styrene

EFEP of styrene was carried out in a 1000 mL kettle with four necks. Prior to polymerization, the reactor was immersed in a

Table I. Conditions for the Micellar Crosslinking Polymerization of Acrylic Acid

Code ^a	AAc (mL)	MBAAm (mg)	PS Emulsion (mL) ^b	N_p ($\times 10^{12}/\text{mL}$)	D_p (nm)	APS (mg)	Frequency (Hz)
N00D4	2.16	2.83	0	0	0	6.12	1
N05D4	2.16	2.83	0.5	0.65	233	6.12	1
N10D4	2.16	2.83	1	1.31	233	6.12	1
N15D4	2.16	2.83	1.5	1.96	233	6.12	1
N40D4	2.16	2.83	4	5.24	233	6.12	1
N10D8	2.16	2.83	1.12	1.31	333	6.12	1
N10D20	2.16	2.83	2.09	1.31	590	6.12	1
N10D24	2.16	2.83	2.76	1.31	696	6.12	1
N10D4A0154	2.16	2.83	1	1.31	233	1.54	1
N10D4A1224	2.16	2.83	1	1.31	233	12.24	1
N10D4F0.1	2.16	2.83	1	1.31	233	6.12	0.1
N10D4F0.5	2.16	2.83	1	1.31	233	6.12	0.5
N10D4F10.0	2.16	2.83	1	1.31	233	6.12	10

^aN: N_p of polystyrene, e.g., N10 is $1.31 \times 10^{12}/\text{mL}$, D: D_p of polystyrene, e.g., D4 is 233 nm, A: the concentration of APS, e.g., A0154 is 1.54 mg of APS, and F: value of frequency. Criteria sample is N10D4, which omitted the terms of A0612 and F1.0 for the variations of concentration of initiator and frequency, respectively.

^bPS Emulsion is polystyrene emulsion prepared by EFEP.

thermostatic water bath. A water-cooled condenser was connected to the reactor and nitrogen was bubbled continuously into the water to remove oxygen while stirring with a one inch paddle at 300 rpm. The reactor containing 700 mL of water was heated to 80°C. Pre-washed styrene (70 mL) was added and equilibrated for 20 min with stirring at 300 rpm. After equilibration, potassium persulfate initiator (0.64 g) was added. Polymerization was conducted at a constant temperature for 5 h. Samples were withdrawn from the reactor at constant time intervals to measure the conversion rate. Each sample was filtered to remove coagulates, kept frozen at -15°C overnight, and melted at room temperature. After melting, the latex separated into two phases. The polystyrene beads settled to the bottom of beaker. The beads were washed with deionized distilled water and methanol, and dried at room temperature for 2 days in a ventilated hood to remove the unreacted monomer and then dried in a vacuum oven at 50°C for 3 days. SEM images of these samples were acquired with a JSM-7001F-LV analytical field emission scanning electron microscope.

Gravimetric Conversion Rate Measurement

Samples for conversion rate measurement were collected at various polymerization time intervals and dropped into 100 mL pre-labeled and pre-weighed beakers. Each beaker was weighed before and after adding the liquid and after drying. Samples were further dried if constant weight was not observed. Gravimetric conversion rate measurements were performed with the assumption that the monomer and polymer were uniformly dispersed in the dispersion system.

$$X_c = \frac{(W_2 - W_0) - (W_1 - W_0) \times C_{\text{initiator}}}{(W_1 - W_0) \times C_{\text{monomer}}} = \frac{W_p}{W_m} \quad (1)$$

In eq. (1), X_c is the conversion rate, W_0 indicates the weight of the empty beaker, W_1 is the weight of the beaker after adding

the initial sample solution, and W_2 is the weight of beaker after drying. $C_{\text{initiator}}$ and C_{monomer} were determined by the weight ratio of the corresponding reactants (initiator 0.64 g and monomer 74.2 g which was from $70 \text{ mL} \times 1.06 \text{ g mL}^{-1}$) to the total weight of charge into the reactor (74.84 g). W_p is the weight of the polymer and W_m is the initial weight of added monomer.

Crosslinking Polymerization of Acrylic Acid with Polystyrene Beads in the Rheometer

Hydrogels were prepared by micellar crosslinking free-radical polymerization. The initial solution consisted of acrylic acid as a monomer, MBAAm, and deionized distilled water. The molar ratio of MBAAm to acrylic acid was kept constant at 0.583×10^{-3} . The solid wt % was fixed to about 23% to reduce the cyclization reaction during gelation.

Measurements of the rheological properties were performed during gelation for 60 min in the time sweep mode in a double-gap cylindrical geometry (DG27, MCR 301, Physica, Anton Paar). The gap between the bottom of cylinder and the bottom of reactor was maintained at 2 mm. The shear strain (amplitude γ) was 1% and the frequency was 1 Hz (frequency sweep measurements were conducted at 0.1, 0.5, 1.0, and 10 Hz). The temperature, which was fixed at 60°C, was controlled by a water bath controller (Julobo, F25). The amount of initial gel solution with each corresponding polystyrene emulsion poured into the DG27 cell was 7 mL. After reaching a temperature of 60°C, 1 mL of the initiator solution was added. The concentration ratios of each reactant are presented in Table I. The time gap between addition of the initiator solution and the starting time of the measurement was 15 s. A total of 30 points were scanned with a time interval of 2 min between each point. This measurement was conducted as a function of the number particle (N_p), the size of the polystyrene particles (D_p), the concentration of APS, and frequency. The

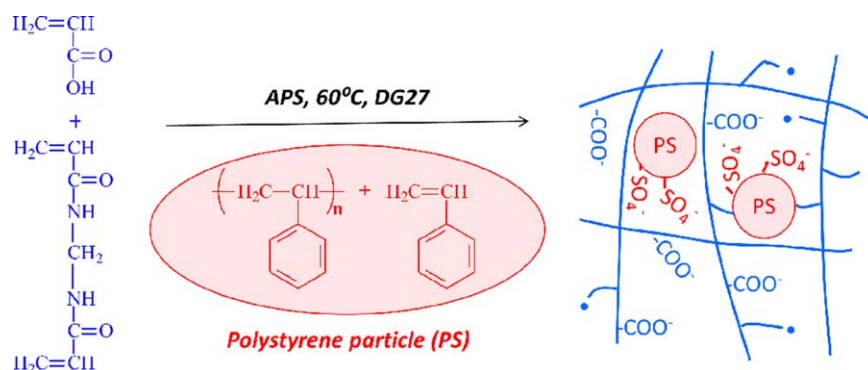


Figure 1. Schematic illustration of micellar crosslinking polymerization of acrylic acid filled with polystyrene particles. [Color figure can be viewed in the online issue, which is available at wileyonlinelibrary.com.]

polymerization and gel structure were schematically illustrated in Figure 1. Polystyrene emulsion used as the solvent at corresponding conversion was taken out of the middle of the reactor without stirring, and thus supernatant styrene monomer was not included in the solvent. Therefore, styrene monomer only exists on the particle phase, except the dissolved styrene in water. Competitive reaction between acrylic acid oligomer and styrene monomer on the aqueous phase would be rarely happened.

RESULTS AND DISCUSSION

EFEP of Styrene

D_p of polystyrene was kinetically controlled in the EFEP process; D_p ranged from 233 nm at 9% conversion to 690 nm at 84% conversion. To prepare these particles, the polymerization rate (R_p) at each time interval versus conversion of the monomer was first plotted as shown in Figure 2. R_p was about $3.7 \times 10^{-8} \text{ mol s}^{-1} \text{ mL}^{-1}$ at 9% conversion and $5.9 \times 10^{-8} \text{ mol s}^{-1} \text{ mL}^{-1}$ at 84% conversion. R_p increased significantly at the beginning of the reaction and then leveled off as the nucleation period ended. R_p decreased above 84% conversion. R_p could be calculated using eq. (2).

$$R_p = [M]_0 \frac{dX_c}{dt} \quad (2)$$

where $[M]_0$ is the feed concentration of the monomer, X_c is the conversion ratio, and t is the polymerization time (in seconds).

N_p was determined using eq. (3).

$$D_p = \left(\frac{6 [M]_0 X_c}{\pi d_p N_p} \right)^{1/3} \quad (3)$$

where d_p is the density of polystyrene (1.05 g/cm^3).²⁹ Equation (3) could be derived from the balance equation: ([gram of monomer]/[density of monomer]) \times conversion = (density of particle) \times (number of particles). The density of styrene is about 0.91 g/cm^3 .²⁹

Polymerization parameters (R_p , N_p , and D_p) for EFEP versus conventional emulsion polymerization are orders of magnitude different. This is from the difference in formation of the micelles and the polymerization behavior.

In conventional emulsion polymerization of styrene, surfactant molecules, such as sodium dodecyl sulfate, are added to the solution at concentrations over the critical micelle concentration to generate micelles as the reaction loci. The number of micelles ranges from 10^{14} to 10^{15} per mL.³⁰ When the radical formed in the aqueous phase diffuses into the micelle, that micelle becomes the particle. As the particle propagates, it becomes unstable and takes more surfactant molecules from other micelles. Thus, during polymerization, styrene monomers that lose surfactant molecules are phase separated and form a supernatant monomer layer if agitation is discontinued.¹⁷

In the case of EFEP, the general route for particle formation is similar to that of emulsion polymerization. However, two points in the nucleation and propagation are different. The first is the mode of formation of the micelle. Surfactant molecules are not added in EFEP. Instead, the monomer molecule itself becomes a part of the surfactant. Styrene is hydrophobic and is minimally solubilized in the aqueous phase. The aqueous solubility of styrene is $10^{-5} \text{ g mL}^{-1}$ of water.²⁹ The solubilized styrene molecules can react with radicals from the decomposed initiator and propagate in the aqueous phase. As the oligomeric radical propagates, the polystyrene portion becomes more hydrophobic, with $-\text{SO}_4^-$ located at the opposite side of the radical in a chain. When the chain reaches a critical length during propagation, it is precipitated and forms micelles with other

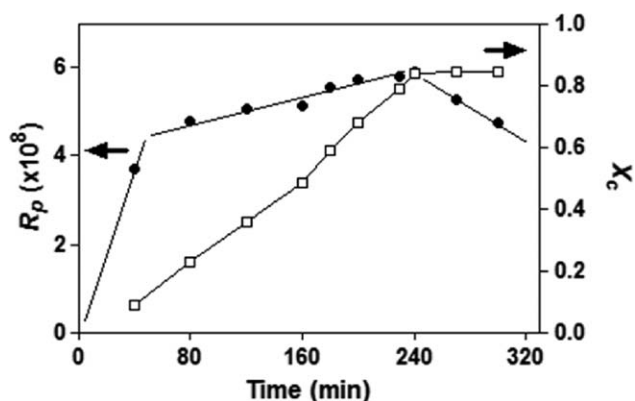


Figure 2. Reaction rate (mol/s/mL, filled circle) and conversion rate of emulsifier-free emulsion polymerization of styrene.

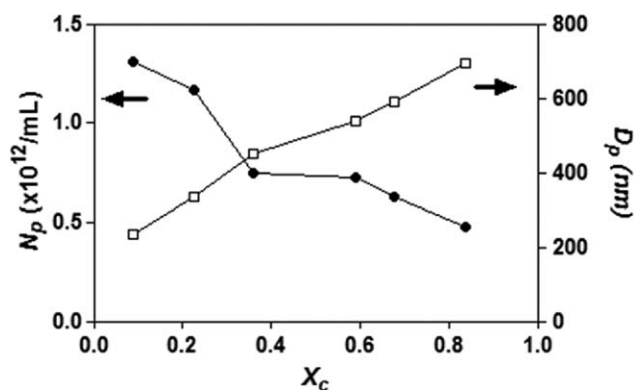


Figure 3. N_p and D_p of polystyrene particle as a function of conversion rate in emulsifier-free emulsion polymerization of styrene.

precipitated oligomeric radicals. When these micelles are formed, the termination reaction occurs. Goodall *et al.*²⁵ measured the molecular weight of polystyrene by gel permeation chromatography. They showed that the amount of polystyrene (for which the molecular weight was about 1000 g mol^{-1}) remained constant throughout the course of polymerization (though the fraction of these molecules decreased as polymerization progressed) and concluded that the molecular weight of the precipitated oligomeric radical was about 500 g mol^{-1} ; after the nucleation period, micelles were not formed—monomers were consumed by particle propagation. The maximum number average molecular weight was reported to be about 10^6 g mol^{-1} .

The critical chain length depends on the hydrophobicity of the monomer. The critical chain length for precipitation of oligomeric radicals to form the micelle is known to be 5–7 for styrene^{31,32} (this value would be 4 if the molecular weight of the precipitated oligomeric radical is 500 g mol^{-1}); for the more hydrophilic methyl methacrylate, the critical chain length is 50.³³ Thus, in EFEP, the micelle number is smaller and the micelle size is bigger than in conventional emulsion polymerization. In EFEP of styrene, N_p (the micelle in EFEP consists of polystyrene radicals) is initially about $5 \times 10^{12}/\text{mL}$, and this value is reduced to 10^{11} to $10^{12}/\text{mL}$.²⁵ In Figure 3, N_p (/mL) ranged from 1.31×10^{12} to 4.75×10^{11} .

The second difference between EFEP and emulsion polymerization is found in the particle growth. In emulsion polymerization, to maintain the stability of the particles during propagation in the aqueous phase, the particles extract surfactant molecules from other empty micelles because the number of micelles is orders of magnitude higher than the number of particles.³⁴ However, in EFEP, particles undergoing propagation become coagulated to maintain their stability in the aqueous phase since the ionic groups are only generated by decomposition of the initiator. Coagulation would thus be related to the rate of radical termination in the aqueous phase, radical capture by the particle, and propagation of the particle. In EFEP, radical termination is significant in the beginning polymerization, but once the nucleation period ends (i.e., when the terminated oligomeric radicals aggregate and form the micelle), the rate of radical capture by the particles is faster than the termination

rate. As the particles are propagated, the rate of propagation becomes faster than the rate of radical capture. In EFEP, the polymerization rate is proportional to the particle size.²⁵ Thus, the propagating particles should undergo coagulation to stabilize the number of $-\text{SO}_4^-$ groups on the surface, and R_p continues to increase until 84% monomer conversion is achieved.

Coagulation between propagating particles does not generate stabilized particles because the ratio of the total surface area to the number of $-\text{SO}_4^-$ groups on the surface would remain the same after coagulation. Instead, coagulation between the propagating particles and the stabilized (no propagation and containing no radicals) particles would result in stabilized particles. Thus, in EFEP, coagulation progresses throughout the entire course of polymerization (Figure 3). Therefore, based on these two main aforementioned features in the EFEP of styrene, large micelles composed of pure polystyrene surfactants and coagulation due to the lack of stability in the aqueous phase results in a continuous reduction of N_p and a rapid increase of D_p .

The particle size as a function of conversion is shown in Figure 4. At 40 min of polymerization ($X_c = 9\%$), the average particle size was 233 nm; the particles erupted due to discharge of volatile materials contained in them when exposed to the vacuum and mounted on the grid of the electron microscope. The hole size decreased as polymerization progressed, and no hole was observed at 200 min of polymerization ($X_c = 68\%$). The formation of hemi-spherical particles and holes on the particle surface arises due to “softness”. It was reported that this phenomenon is only observed in the beginning of EFEP of styrene. These anomalous particles have never been observed in EFEP of hydrophilic monomers such as ethyl acrylate, vinyl acetate, and butyl acrylate.³⁵

Micellar Crosslinking Polymerization of Acrylic Acid as a Function of Polystyrene Loading Level

To chemically incorporate polystyrene particles into the poly (acrylic acid) (PAAc) network, copolymerization between these two different types of polymers must be achieved. In addition to the assumption that precipitated (phase separated) cross-linked PAAc chains can react with polystyrene particles, whether linear or branched PAAc chains react with polystyrene before the infinite molecule is formed should be clarified. Several studies^{27,28,37–43} reported copolymerization between hydrophobe molecules in the micelles and that the formation of hydrophilic oligomeric radicals was possible.

Dowling and Thomas³⁹ prepared acrylamide and styrene block copolymers by micellar polymerization. In their study, the hydrophobe was composed of 14–30 styrene molecules, as determined by Poisson fluorescence quenching kinetics. Peer⁴⁴ reported the copolymerization of lauryl methacrylate (>1 mol %) and acrylamide with a mixed surfactant consisting of sodium dodecyl sulfate and dodecyl penta(oxyethylene glycol) monoether. In this copolymerization, the sequence length of lauryl methacrylate in the copolymer increased as the feed concentration of acrylamide increased. Candau *et al.*⁴⁵ reported that acrylamide and sodium acrylate co-existed at the palisade layer of the micelle, and these species could be copolymerized by microemulsion polymerization. They³⁸ also reported that the

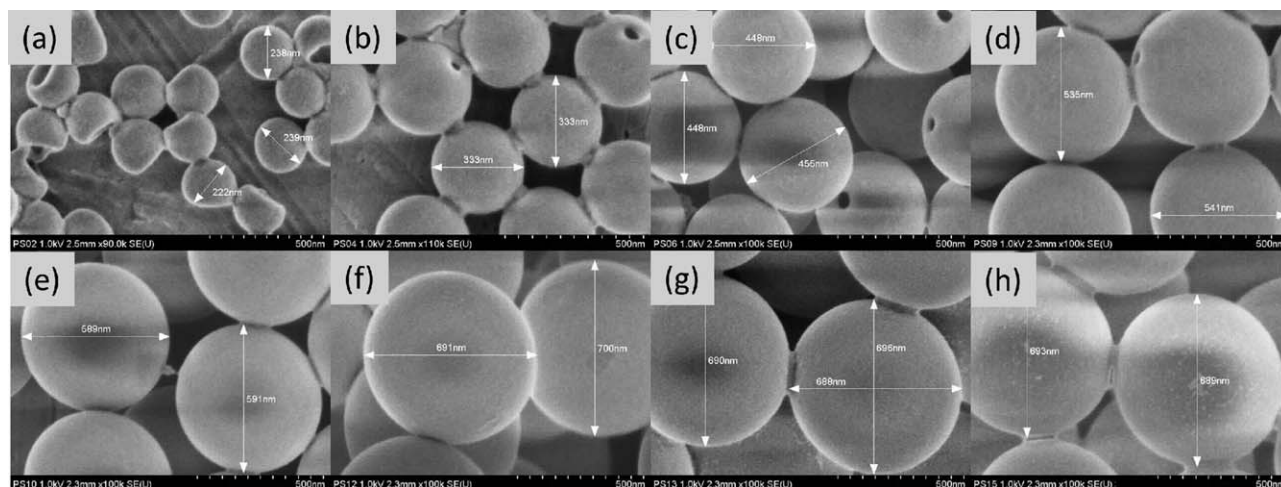


Figure 4. SEM pictures of polystyrene particle prepared at (a) 40 min ($X_c = 0.09$, 233 nm), (b) 80 min ($X_c = 0.23$, 333 nm), (c) 120 min ($X_c = 0.36$, 450 nm), (d) 160 min ($X_c = 0.48$, 536 nm), (e) 200 min ($X_c = 0.68$, 590 nm), (f) 240 min ($X_c = 0.84$, 696 nm), (g) 270 min ($X_c = 0.84$, 693 nm), and (h) 300 min ($X_c = 0.84$, 691 nm). Particle size distribution was below 1.10.

feed composition of the hydrophobe was the same in the copolymer prepared by linear micellar copolymerization.

Similarly, micellar crosslinking copolymerization between polystyrene particles and PAAc with MBAAm was possible in the present system. The induction period varied as a function of the polystyrene emulsion loading level [Figure 5(a)]. The induction period for pure PAAc crosslinking polymerization was 3 min. However, induction was delayed as the polystyrene particles were incorporated. In the case of N05D4, which included 0.5 mL of polystyrene emulsion (6.50×10^{11} particles) as shown in Table I, the induction period was 4 min. Induction periods of 6, 10, and 12 min were, respectively, required for N10D4, N15D4, and N20D4. The delayed gelation time was generally proportional to the loading level of polystyrene particles.

In the process of forming the network, trifunctional molecules composed of PAAc radicals and more than two pendant (MBAAm) molecules are generated; the infinite molecule is formed by bridging of these molecules with each other.⁴⁶ When the infinite molecule is formed, G' increases significantly and gelation is observed (water soluble molecules are precipitated). During the induction period, PAAc radicals would be consumed by the particles that are propagated after reaction with styrene monomers on the particles; encapsulated radicals rarely exit the large particle (>200 nm). Thus, despite the high N_p , it could be more difficult to form the infinite molecule.

After the induction period, the infinite molecule was propagated with separated branched molecules. This propagation was also interrupted by polystyrene particles. Upon addition of 4 mL of polystyrene emulsion ($N_p = 5.24 \times 10^{12}$), the slope of the time versus G' plot decreased from 10.7 to 3.6 [Figure 5(b)]. However, in the deceleration period [Figure 5(c)], G' of N40D4 increased remarkably. After formation of the network, unreacted radicals of trapped branched molecules or of the infinite molecule should react; instead, their reaction rate was slowed due to immobilization.⁴⁷ Thus, it could be inferred that the rate of the

reaction between the radicals increased as more particles including styrene were incorporated.

As shown in Figure 5, the G' value of N10D4 ($N_p = 1.31 \times 10^{12}$) increased remarkably compared to that of the other samples. This might be attributed to competition between two possible opposite effects induced by incorporation of the polystyrene particles. First, the viscosity of the solution would increase. Styrene monomers dissolved in the reaction media could react with the PAAc chains, thereby increasing the compatibility between the particles and PAAc. The increased viscosity of the liquid surrounding the polystyrene particles would decrease the mobility of the PAAc chain and decrease the rate of termination between PAAc radicals because the termination reaction is controlled by diffusion. Kubota⁹ compared the curing rate of mono-chlorostyrene, *tert*-butylstyrene, styrene, and vinyltoluene with an inert thermoplastic additive. In that study, the viscosity of the styrene solution changed from 300 to 2000 cp upon addition of 9.8% cellulose acetate butyrate. It was concluded that the increased viscosity reduced the termination reaction and promoted the curing rate. However, as the second opposite effect, it was suggested that the amount of styrene to be cured would decrease as styrene is absorbed or occluded in the aggregates when the additive precipitates. This would decrease the final conversion of styrene, as observed in Figure 5(a).

If the amount of acrylic acid available during crosslinking polymerization is reduced, the mesh size of the hydrogel would also decrease. Thus, G' would increase. However, the rate of crosslinking decreased for all filled samples, despite the fact that two positive effects (an increase of the viscosity and a decrease of the mesh size) were possible. This could be attributed to the large size of the branched molecules. The size of the branched molecule may be reduced as the concentration of the crosslinking agent is increased.^{46,48} More compact branched molecules may result in a faster crosslinking rate.⁴⁶ If polystyrene particles are incorporated into these branched molecules, the size of

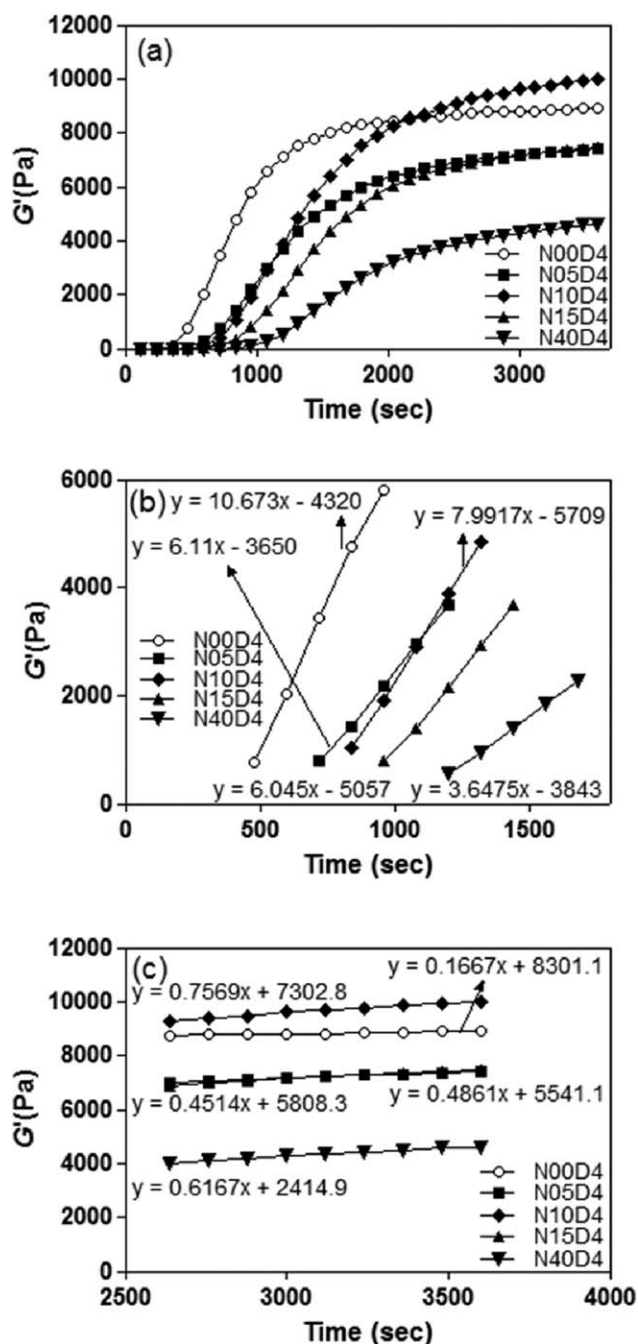


Figure 5. (a) G' during the micellar crosslinking polymerization of acrylic acid ($N_p = 0$ to 5.24×10^{12} /mL), (b) slopes at propagation period dependent on N_p , and (c) slopes at deceleration period dependent on N_p .

branched molecules will increase significantly and the crosslinking rate will decrease. In this case, the crosslinking rate and G'_{\max} should decrease as the polystyrene particles are incorporated. However, as mentioned previously, G'_{\max} of N10D4 was much higher than that of N00D4.

Presumably, there is an optimal ratio between the surface area of the particles and the concentration of radicals in the solution at a fixed ratio of acrylic acid to MBAAm (in the latter part of initiation, G'_{\max} decreased as the concentration of the initiator decreased). The number of radicals generated in the solution

(Table I) was 4.04×10^{18} /mL, and the N_p of N10D4 was 1.31×10^{12} /mL; the ratio of radicals to N_p was 3.08×10^6 . In this case, the average number of radicals per unit area (nm^2) of particles is 18.03 (this is equal to 5.54×10^{-2} nm^2 /radical) if all the radicals enter into the particles. This ratio of bonding sites per nm^2 of filler surface is two orders of magnitude higher than the ratio reported by Edwards.⁴⁹ In that study of the terminally brominated liquid polybutadiene matrix system, the optimal bonding site per nm^2 of filler surface ratio for achieving the strongest bonding in vulcanizates was 0.2. At a ratio of 0.82 bonding sites per nm^2 , the tensile strength and elongation at break were reduced. Therefore, if this ratio of 0.2 is applied to the present system, about 1.1% of the total radicals enter into the particles. This low fraction is attributed to the fact that most radicals are from the immobilized network chain, or may be due to the difference in the chemicals, crosslinking route, and filler types. Further study would be required to clarify the relationship between N_p , the number of radicals, and the concentrations of MBAAm and acrylic acid to achieve the strongest bonding between the surface of the particles and the radicals.

As shown in Figure 6, the value of $\tan\delta$ increased as N_p increased (Figure 6). In other words, G'' (the viscous modulus; as the energy dissipation term to G') was relatively higher when compared to the case of the unfilled sample (N00D4). It is thus inferred that physical interaction (or crosslinking) between the particles and PAAc was induced, and the ratio of the viscosity to storage property increased.²⁷ This physical crosslinking and the larger surface of the particles (proportional to N_p) are believed to interrupt chemical crosslinking. The rate of entry of radicals into the particle is proportional to the total surface area of the particles.²⁸ This rate of entry into the particle would increase as N_p increased, thereby delaying gelation. The G^*/G^*_{\max} value of each sample indicates the rate of crosslinking (Figure 7).

Micellar Crosslinking Polymerization of Acrylic Acid as a Function of Particle Size

To evaluate the effect of the particle size on the crosslinking efficiency, N_p was fixed to 1.31×10^{12} /mL and G' , $\tan\delta$, and G^*/G^*_{\max} were monitored during the polymerization. The respective particle sizes of N10D4, N10D8, N10D20, and

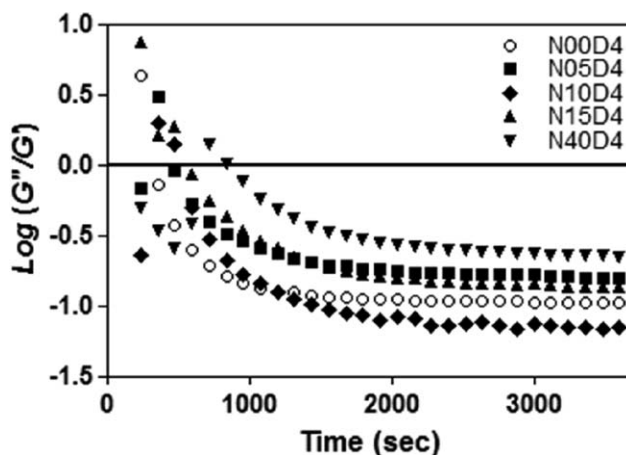


Figure 6. Dependence of damping factors on the N_p of polystyrene during the micellar crosslinking polymerization of acrylic acid.

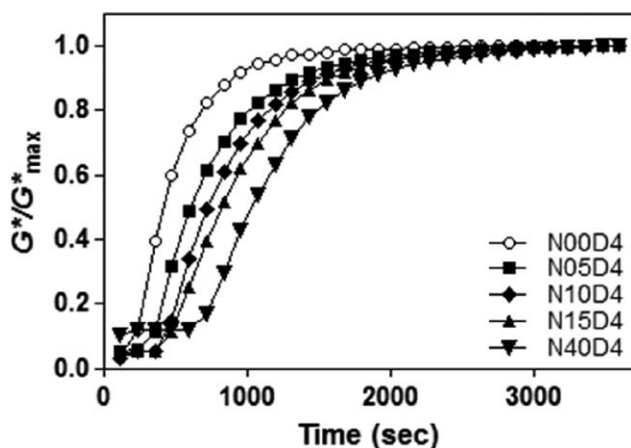


Figure 7. G^*/G^*_{\max} plot as a function of N_p of polystyrene during the micellar crosslinking polymerization.

N10D24 were 233, 333, 590, and 690 nm. The induction period decreased, and the rate of network formation in the propagation period and the rate of radical capture in the deceleration period generally increased with increasing particle size (Figure 8). This was reversed in a view of the most efficient crosslinking to the surface area of particles, against at the previous part of crosslinking rate and the number of particles. It could not be finalized clearly, but we thought that the most optimized total surface area of particles for the most efficient crosslinking was more closed by in N10D20 sample.

Generally, two exceptions to this behavior, which G' increased faster as the particle size was bigger, were observed—(1) the rate of reaction did not follow this size dependence in the case of N10D4 and (2) the rate of radical capture in the deceleration period was significantly lower in the case of N10D24 compared to the others.

The exception in the case of N10D4 is attributed to the particle “softness”. The dispersity of soft particles is better than that of rigid particles. For softer particles, the surface is rougher and the porosity is higher.⁵⁰ Thus, more PAAc chains would react with the soft particles. This softness could cause a reduction of the induction period. As shown in Figure 8(a), the induction period was longer for N10D4 compared to the other samples, but G' increased at a similar point as observed for N10D20. However, this exception did not correspond to the propagation and deceleration periods.

The second exception is the low slope for N10D24 in the deceleration period. The slope was 0.55, which is much lower than the values of 0.83 for N10D20 and N10D8, and 0.76 for N10D4. The distance between particles would decrease and the probability for the attractive hydrophobic interaction would be higher for larger particles. In this measurement, coagulation would be more significant for the 696 nm particles, resulting in a decrease of the total surface area of the particles.

$\text{Tan}\delta$ also increases for larger particles. Increasing the total surface area of the particles results in an increase of the ratio of viscosity to G' . In the case of the poly(acrylamide) network filled with *N*-octylacrylamide as a hydrophobe, increasing the

number of hydrophobes from 9 to 30 induced an increase in the elongation ratio at break from 125% to 250%.²⁷ Candau and colleagues^{28,37,43} evaluated the effect of dilution of poly(acrylamide) solution with dihexylacrylamide as a hydrophobe on the hydrophobic interaction between the hydrophobes by varying the number and size of hydrophobes in the micellar polymerization system. In their report, the zero-shear viscosity was dependent on the number and size of hydrophobes in the unentangled semi-dilute region, and was independent of the

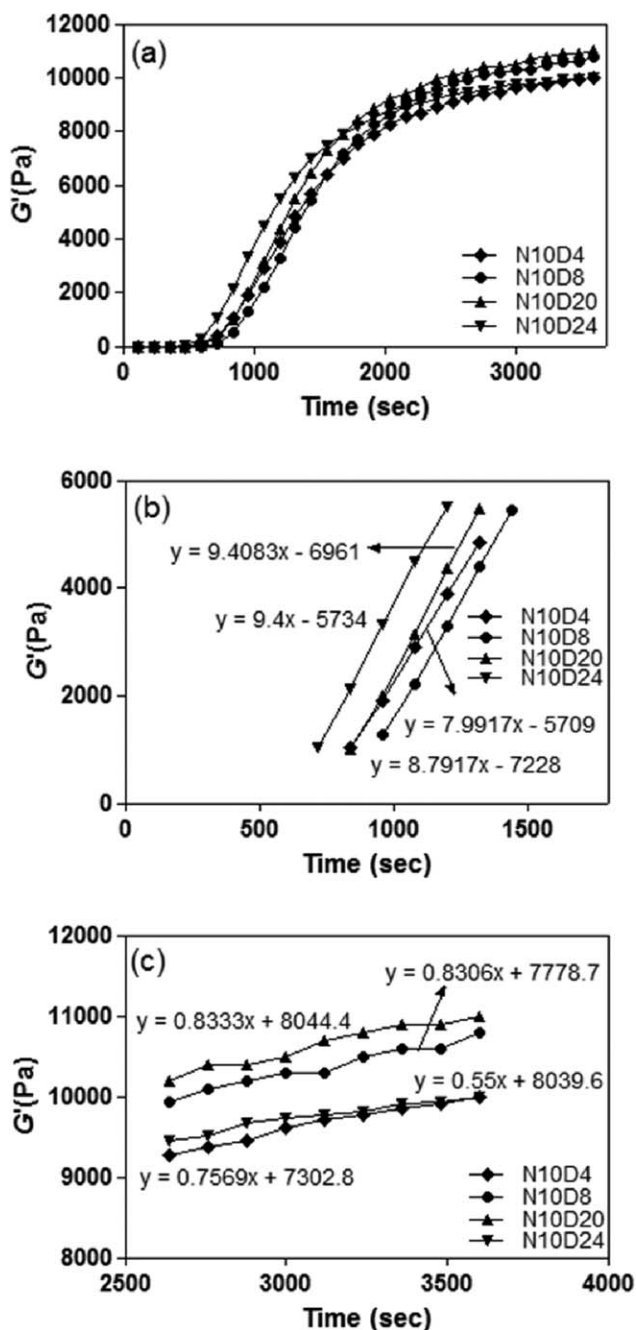


Figure 8. (a) G' during the micellar crosslinking polymerization of acrylic acid [D_p (nm) = 233 to 696], (b) slopes at propagation period dependent on D_p , and (c) slopes at deceleration period dependent on D_p .

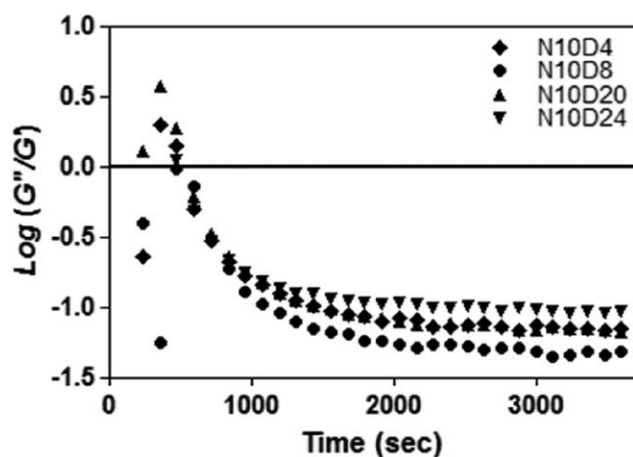


Figure 9. Dependence of damping factors on the D_p of polystyrene during the micellar crosslinking polymerization of acrylic acid.

number and size of hydrophobes in the entangled region, but dependent on the biquadrate of the polymer concentration.

Herein, the size of the polystyrene particles was found to affect the shear properties; notably, $\tan\delta$ increased as the size of the polystyrene particles increased (Figure 9). It was proposed that the physical interaction between the particles and the PAAc, which included a small fraction of styrene in the chain, could increase the ratio of G'' to G' .²⁷

The behavior of G' and $\tan\delta$ in the induction period and the slopes of the curves for each sample in the propagation and deceleration periods could be confirmed from the data in Figure 10, which shows the rate of crosslinking polymerization of acrylic acid filled with polystyrene particles.

Micellar Crosslinking Polymerization of Acrylic Acid as a Function of APS Concentration

The influence of the concentration of APS (as an initiator) on the efficiency of crosslinking was investigated. The induction period was shorter when higher concentrations of APS were used [Figure 11(a)]. During the propagation period [Figure 11(b)], the slope of time versus G' was proportional to the con-

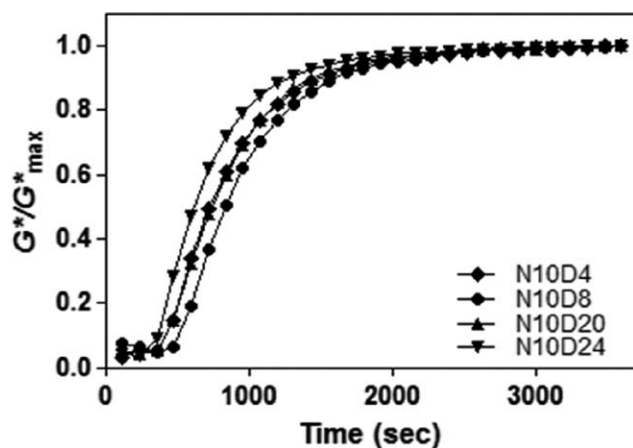


Figure 10. G^*/G^*_{\max} plot as a function of D_p of polystyrene during the micellar crosslinking polymerization.

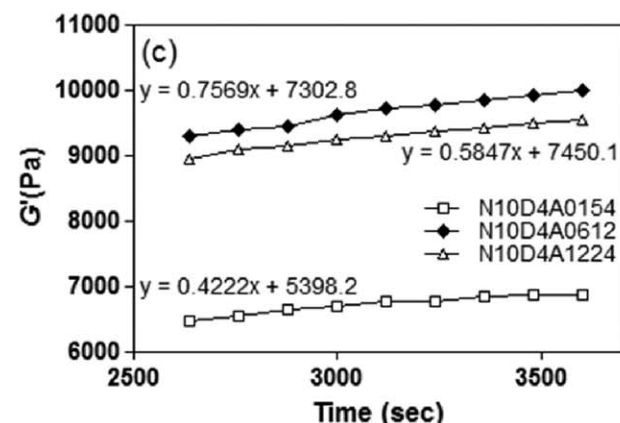
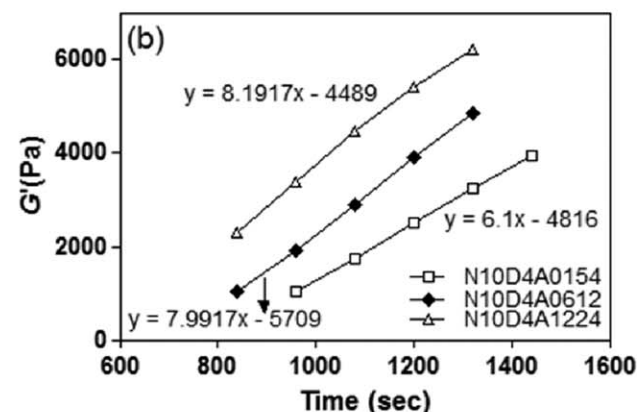
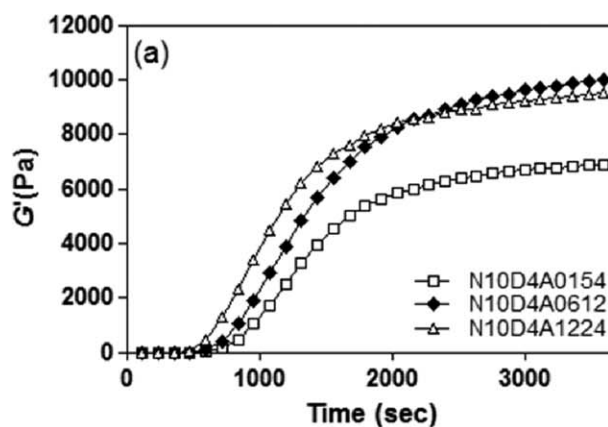


Figure 11. (a) G' during the micellar crosslinking polymerization of acrylic acid (APS (mg) = 0.154–12.24), (b) slopes at propagation period dependent on [APS], and (c) slopes at deceleration period dependent on [APS].

centration of APS, i.e., 8.19, 7.99, and 6.10 for 12.24, 6.12, and 1.54 mg of APS, respectively. However, this order did not correspond to the deceleration period [Figure 11(c)]. The steepness of the slope ranked in the order: N10D4A0612 > N10D4A1224 > N10D4A0154. This is attributed to the most effective bondings per unit area of particles as mentioned previously.

The $\tan\delta$ values were higher as the concentration of APS was lower (Figure 12). The rate of the crosslinking polymerization

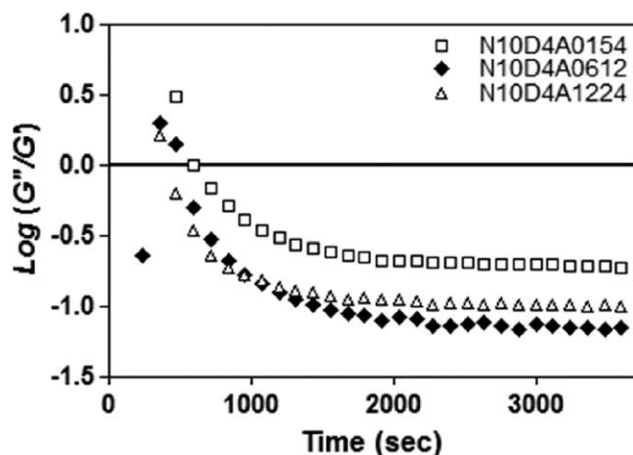


Figure 12. Dependence of damping factors on the concentration of APS of polystyrene during the micellar crosslinking polymerization of acrylic acid.

was slightly affected by the APS concentration (Figure 13), but was still faster at high APS concentration.

In the free-radical crosslinking polymerization, the molar ratio of the monomer to the crosslinking agent is important for determining the mesh size of the hydrogel. The MBAAm molecules contribute to imparting functionality to the molecules, especially trifunctional molecules.⁴⁶ The main role of MBAAm in crosslinking is to induce the formation of junctions in the

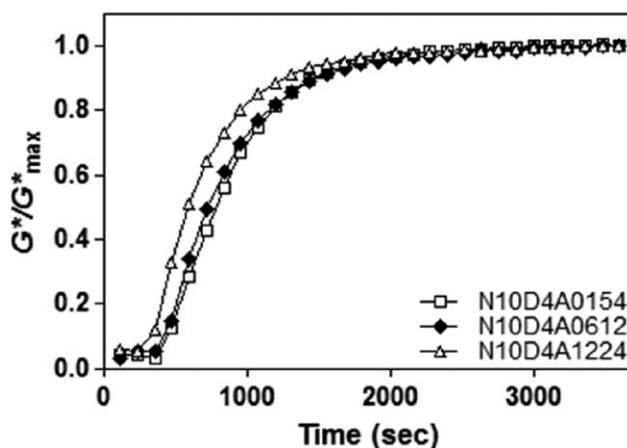


Figure 13. G^*/G^*_{max} plot as a function of the concentration of APS during the micellar crosslinking polymerization of N10D4.

linear PAAc chain. Thus, increasing the concentration of MBAAm reduces the size of the branched molecules prior to completion of gelation, which results in faster crosslinking polymerization.

In the formation of trifunctional molecules, the length of the linear PAAc chain can be determined by the ratio of [AAc] and the molar concentration of APS.⁵¹ Thus, even if the MBAAm concentration is high, the size of the branched molecule becomes larger if the concentration of APS is much lower. This

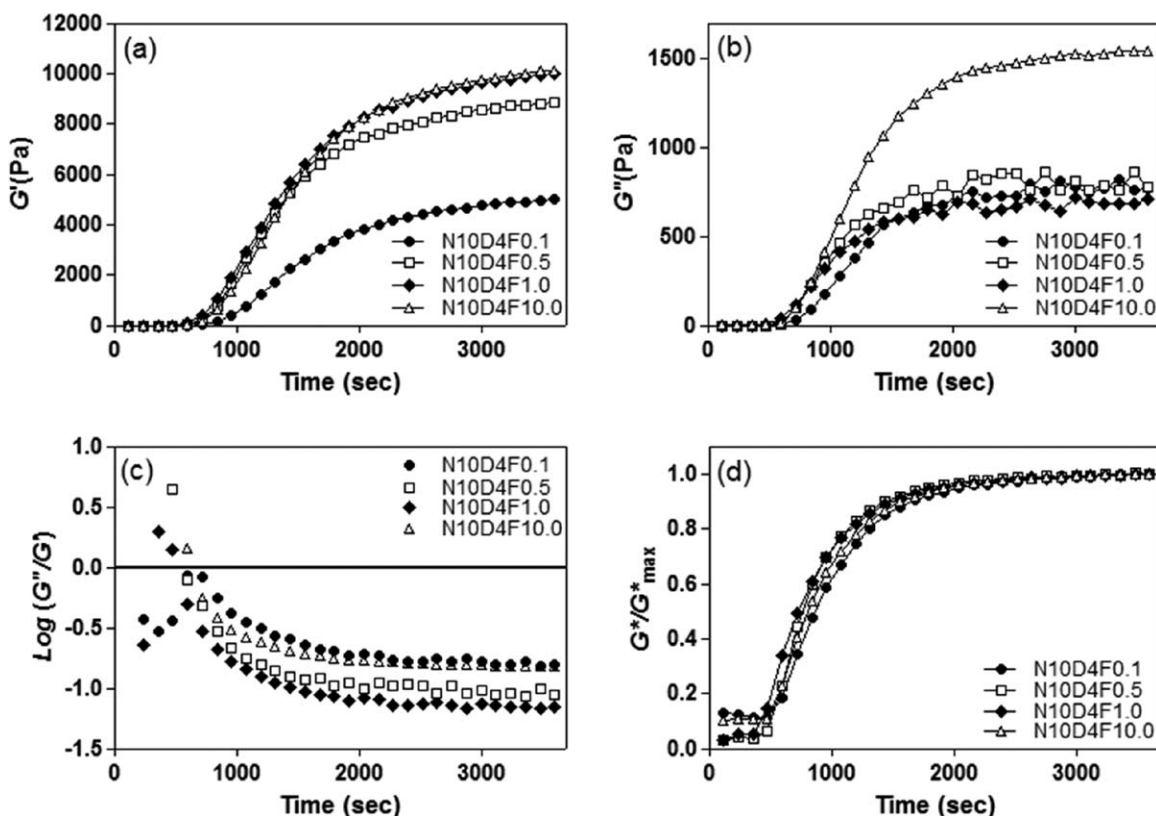


Figure 14. Dependence of G' , G'' , damping factor, and G^*/G^*_{max} on the frequency, 0.1, 0.5, 1.0, and 10.0 Hz during the micellar crosslinking polymerization of N10D4.

results in a low crosslinking polymerization rate, and highlights the effect of low (MBAAm).

During crosslinking polymerization in the system filled with polystyrene particles, a lower concentration of APS results in a decrease in the average number of bonds per unit area (nm^2) of the particle surface. Moreover, due to the longer distance between the junctions in the PAAc chain, the distance between the junction of PAAc and particle surface would be longer. Thus, the mobility of the particle would be higher, and $\tan\delta$ would increase.

Micellar Crosslinking Polymerization of Acrylic Acid as a Function of Frequency

The G' , G'' , $\tan\delta$, and G^*/G^*_{\max} values of N10D4 (polystyrene particle-filled PAAc hydrogel, $N_p = 1.31 \times 10^{12}/\text{mL}$, $D_p = 233 \text{ nm}$) during crosslinking polymerization were plotted at frequencies of 0.1, 0.5, 1.0, and 10.0 Hz. G' was not highly sensitive to frequency in the range of 0.5–10 Hz, but decreased significantly at 0.1 Hz [Figure 14(a)]. G''_{\max} ranged between 600 and 900 Pa, but reached a value of 1500 Pa at 10 Hz [Figure 14(b)]. Thus, $\tan\delta$ was high at 0.1 Hz and 10 Hz, and low at 0.5 Hz and 1.0 Hz [Figure 14(c)]. The curves of G^*/G^*_{\max} at all frequencies converged into one curve.

G'' increased at high frequency (10 Hz). However, the dynamic viscosity (G''/Hz) at 10 Hz was lower than at other frequencies (not plotted). As the shear rate increased, the formation of cluster structures composed of branched molecules and polystyrene particles would be interrupted, resulting in less occlusion of the structure, thereby increasing the viscosity. Thus, at a high shear rate, the dynamic moduli or viscosity of the suspension was determined by the nature of the crosslinking PAAc and the effect of the particles was less significant.

The point at which $\tan\delta$ is equal to 1.0 is called the “gel point”; the Winter–Chambon criterion is valid at this point.^{52,53} For N10D4, this point was observed near 11 min of polymerization ($\log(G''/G') = 0$). However, the gel point does not always occur at $\tan\delta = 1$, especially in multicomponent systems. Chiou *et al.*⁵⁴ reported validity of the Winter–Chambon criterion during thiol-ene formulation using fumed silica, where the surface contained *n*-octyl groups with three $-\text{O}^-$ moieties and dimethyl groups with two $-\text{O}^-$ moieties. In this case, the gel point was observed at $\tan\delta = 1$ for the methyl terminated silica, but not for the octyl modified silica. Failure of the gel point to occur at $\tan\delta = 1$ could be attributed to abnormal growth kinetics, a highly polydispersed structure,^{55,56} or phase separation before the gel point.⁵⁷

Therefore, it can be deduced that in the present system, before the gel point where the infinite molecule was formed, coagulation of polystyrene particles was not significant and the particles were evenly dispersed, the branched PAAc chains were not precipitated, and all the G' and G^*/G^*_{\max} curves were superimposable.

CONCLUSIONS

To isolate the effect of polystyrene particles on the crosslinking polymerization of acrylic acid, the rheological parameters, G' ,

$\tan\delta$, and G^*/G^*_{\max} were measured during crosslinking polymerization at 60°C over the course of 1 h using a double-gap cylindrical system (DG27) and evaluated as a function of N_p , D_p , the concentration of APS, and frequency.

Polystyrene particles were generated by EFEP of styrene, where the particle size was kinetically controlled. Particles with sizes of 233, 333, 590, and 696 nm were thus obtained. N_p was calculated based on these particle sizes.

Incorporation of polystyrene particles into the acrylic acid system reduced the rate of crosslinking polymerization with no improvement of the rheological properties of the hydrogel. However, exceptional enhancement of the rheological properties of the hydrogel was achieved when 1 mL of an emulsion containing 1.31×10^{12} polystyrene particles was incorporated into the polymerization system. The best ratio of bonding sites per unit area of the particle surface is proposed to be 0.2 bonding sites per nm^2 .

Larger particles resulted in the formation of stronger hydrogels with fixed N_p . The particles were more evenly dispersed and the PAAc chains could be more deeply embedded into the softer particles.

Crosslinking progressed more efficiently at higher APS to acrylic acid concentration ratios. However, at ratios exceeding 8.52×10^{-4} , no significant enhancement of G' was achieved, while G' increased more slowly in the deceleration period.

In the measurement of $\tan\delta$ for N10D4 as a function of frequency, 0.1, 0.5, 1.0, and 10.0 Hz, the gel point was observed at the point where $G' = G''$, which obeyed the Winter–Chambon criterion. Thus, it could be deduced that the polystyrene-filled micellar crosslinking polymerization of acrylic acid progressed successfully without phase transition prior to gelation, and the polydispersity was not significant.

REFERENCES

1. Fan, J.; Shi, Z.; Lian, M.; Li, H.; Yin, J. *J. Mater. Chem. A* **2013**, *1*, 7433.
2. Zhang, H.; Zhai, D.; He, Y. *RSC Adv.* **2014**, *4*, 44600.
3. Oliveira, M. B.; Luz, G. M.; Mano, J. F. *J. Mater. Chem. B* **2014**, *2*, 5627.
4. Yuan, H.; Bai, H.; Liu, L.; Lv, F.; Wang, S. *Chem. Commun.* **2015**, *51*, 722.
5. Sereshti, H.; Samdi, S.; Asgari, S.; Karimi, M. *RSC Adv.* **2015**, *5*, 9396.
6. Merino, S.; Martin, C.; Kostarelos, K.; Prato, M.; Vazquez, E. *ACS Nano* **2015**, *5*, 4686.
7. Dong, G.; Kuan, C.; Subramaniam, S.; Zhao, J.; Sivashubramaniam, S.; Chang, H.; Lin, F. *Mater. Sci. Eng. C* **2015**, *49*, 691.
8. Lem, K. W.; Han, C. D. *J. Appl. Polym. Sci.* **1983**, *28*, 3185.
9. Kubota, H. *J. Appl. Polym. Sci.* **1975**, *19*, 2279.
10. Dutta, A.; Ryan, M. E. *J. Appl. Polym. Sci.* **1979**, *24*, 635.
11. Ng, H.; Manas-Zloczower, I. *Polym. Eng. Sci.* **1993**, *33*, 211.

12. Pingsheng, H.; Chune, L. *J. Appl. Polym. Sci.* **1991**, *43*, 1011.
13. De Miranda, M. I. G.; Tomedi, C.; Bica, C. I. D.; Samios, D. *Polymer* **1997**, *38*, 1017.
14. Warson, H. In *Applications of Synthetic Resin Latices*; Wason, H.; Finch, C. A. Eds.; John Wiley and Sons: England, **2001**; Vol. 1, Chapter 6.
15. Cai, J. J.; Salovey, R. *Polym. Eng. Sci.* **2000**, *40*, 118.
16. Cai, J. J.; Salovey, R. *Polym. Eng. Sci.* **1999**, *39*, 1696.
17. Flory, P. J. *Principles of Polymer Chemistry*; Cornell University Press: Ithaca, **1953**, Chapter 5, p 203.
18. Vanderhoff, J. W.; Van den Hull, H. J.; Tausk, R. J. M.; Overbeek, J. T. G. In *Clean Surfaces: Their Preparation and Characterization for Interfacial Studies*; Goldfinger, E. Ed., Dekker: New York, **1970**, p 15.
19. Bovey, F. A.; Kolthoff, I. M.; Medalia, A. I.; Meehan, E. J. *Emulsion Polymerization*, Interscience: New York, **1955**.
20. Van den Hull, H. J.; Vanderhoff, J. W. *Br. Polym. J.* **1970**, *2*, 121.
21. Goodall, A. R.; Hearn, J.; Wilkinson, M. C. *Br. Polym. J.* **1978**, *10*, 141.
22. Goodwin, J. W.; Ottewill, R. H.; Pelton, R. *Colloid Polym. Sci.* **1979**, *257*, 61.
23. Munro, D.; Goodall, A. R.; Wilkinson, M. C.; Randle, K.; Hearn, J. *J. Colloid Interf. Sci.* **1979**, *68*, 1.
24. Song, A.; Poehlein, G. W. *J. Colloid Interf. Sci.* **1989**, *128*, 486.
25. Goodall, A. R.; Wilkinson, M. C.; Hearn, J. *J. Polym. Sci. Part A Polym. Chem.* **1977**, *15*, 2193.
26. Williams, D. J.; Bobalek, E. G. *J. Polym. Sci. A-1* **1966**, *4*, 3065.
27. Abdurrahmanoglu, S.; Can, V.; Okay, O. *Polymer* **2009**, *50*, 5449.
28. Hill, A.; Candau, F.; Selb, J. *Macromolecules* **1993**, *26*, 4521.
29. Brandrup, J.; Immergut, E. H.; Grulke, E. A. *Polymer Handbook*; Wiley-Interscience: New York, **1999**.
30. Smith, W. V. *J. Am. Chem. Soc.* **1948**, *70*, 3695.
31. Guillaume, J. L.; Pichot, C.; Guillot, J. *J. Polym. Sci. Part A Polym. Chem.* **1990**, *28*, 119.
32. Vanderhoff, J. W. *J. Polym. Sci. Polym. Symp.* **1985**, *72*, 161.
33. Goodall, A. R.; Wilkinson, M. C.; Hearn, J. In *Polymer Colloids II*; Fitch, R. M. Ed.; Plenum: New York, **1980**, p 629.
34. Hermanson, K. D.; Kaler, E. W. *Macromolecules* **2003**, *36*, 1836.
35. Fitch, R. M. Paper Presented at NATO Meeting on Polymer Colloids, Trondheim, **1975**.
36. Miquelard-Garnier, G.; Demoures, S.; Creton, C.; Hourdet, D. *Macromolecules* **2006**, *39*, 8128.
37. Volpert, E.; Selb, J.; Francoise, C. *Polymer* **1998**, *39*, 1025.
38. Volpert, E.; Selb, J.; Candau, F. *Macromolecules* **1996**, *29*, 1452.
39. Dowling, K. C.; Thomas, J. K. *Macromolecules* **1990**, *23*, 1059.
40. Ezzel, S. A.; Hoyle, C. E.; Creed, D.; McCormick, C. L. *Macromolecules* **1992**, *25*, 1887.
41. Hill, A.; Candau, F.; Selb, J. *Prog. Colloid Polym. Sci.* **1991**, *84*, 61.
42. Candau, F.; Jimenez Regalado, E.; Selb, J. *Macromolecules* **1998**, *31*, 5550.
43. Jimenez Regalado, E.; Selb, J.; Candau, F. *Macromolecules* **1999**, *32*, 8580.
44. Peer, W. J. *Adv. Chem. Ser.* **1989**, *223*, Chapter 20, p 381.
45. Candau, F.; Zekhnini, Z.; Durand, J. P. *J. Colloid Interf. Sci.* **1986**, *114*, 398.
46. Kim, B.; Hong, D.; Chang, W. V. *J. Appl. Polym. Sci.* **2015**, *132*, 42195.
47. Kim, B.; Hong, D.; Chang, W. V. *J. Appl. Polym. Sci.* **2014**, *131*, 41026.
48. Keskinel, M.; Okay, O. *Polym. Bull.* **1998**, *40*, 491.
49. Edwards, D. C. *J. Mater. Sci.* **1990**, *25*, 4175.
50. Cai, J. J.; Salovey, R. *Polym. Eng. Sci.* **2001**, *41*, 1853.
51. Malkin, A. Y.; Kulichikhin, S. G.; Emel'yanov, D. N.; Smetanina, I. E.; Ryabokon, N. V. *Polymer* **1984**, *25*, 778.
52. Winter, H. H. In *Encyclopedia of Polymer Science and Engineering*, John Wiley & Sons: New York, **1989**.
53. Winter, H. H.; Chambon, F. *J. Rheol.* **1986**, *30*, 367.
54. Chiou, B.; Raghavan, S. R.; Khan, S. A. *Macromolecules* **2001**, *34*, 4526.
55. Ilvasky, M.; Bubenikova, Z.; Bouchal, K.; Fahnrich, J. *Polymer* **1996**, *37*, 3851.
56. Ilvasky, M.; Bubenikova, Z.; Bouchal, K.; Nedbal, J.; Fahnrich, J. *Polym. Bull.* **1999**, *42*, 465.
57. Izuka, A.; Winter, H. H.; Hashimoto, T. *Macromolecules* **1997**, *30*, 6158.